HHS Public Access

Author manuscript

Exp Eye Res. Author manuscript; available in PMC 2022 January 01.

Published in final edited form as:

Exp Eye Res. 2021 January ; 202: 108370. doi:10.1016/j.exer.2020.108370.

An Efficient Inducible RPE-Selective Cre Transgenic Mouse Line

Ming Chen[a], **Lily Kim**[a], **Carolyn W. Lu**[a], **Hong Zeng**[b], **Douglas Vollrath**[a,*]

[a]Department of Genetics, Stanford University School of Medicine, Stanford, CA, United States, 94305

[b]Transgenic, Knockout, and Tumor Model Center, Stanford University School of Medicine, Stanford, CA, United States, 94305

Abstract

Cre-mediated modulation of gene function in the murine retinal pigment epithelium (RPE) has been widely used, but current postnatal RPE-selective Cre driver lines suffer from limited recombination efficiency and/or ectopic or mosaic expression. We sought to generate a transgenic mouse line with consistently efficient RPE-selective Cre activity that could be temporally regulated. We used φC31 integrase to insert a DNA construct encoding a human *BEST1* promoter fragment driving a Cre recombinase estrogen receptor fusion (*BEST1-CreERT2*) at the *Rosa26* locus of C57BL/6J mice. *Rosa26*$^{BEST1\text{-}CreERT2}$ mice were bred with a tdTomato reporter line and to mice with a Cre-conditional allele of *Tfam*. 4-hydroxytamoxifen or vehicle was delivered by four consecutive daily intraperitoneal injections. tdTomato was robustly expressed in the RPE of mice of both sexes for inductions beginning at P14 (males 90.7±4.5%, females 84.7±3.2%) and at 7 weeks (males 84.3±7.0%, females 82±3.6%). <0.6% of Muller glia also expressed tdTomato, but no tdTomato fluorescence was observed in other ocular cells or in multiple non-ocular tissues, with the exception of sparse foci in the testis. No evidence of retinal toxicity was observed in mice homozygous for the transgene induced beginning at P14 and assessed at 7 to 10 months. RPE-selective ablation of *Tfam* beginning at P14 led to reduced retinal thickness at 8 months of age and diminished retinal electrical responses at 12 months, as expected. These findings demonstrate that we have generated a mouse line with consistently efficient, tamoxifen-mediated postnatal induction of Cre recombination in the RPE and a small fraction of Muller glia. This line should be useful for temporally regulated modulation of gene function in the murine RPE.

Keywords

retinal pigment epithelium; Cre recombinase; tdTomato; inducible expression; tamoxifen

*Corresponding Author: vollrath@stanford.edu.

Conflicts of interest: The authors have declared they have no competing interests.

Declarations of interest: none

1. Introduction

The retinal pigment epithelium (RPE) performs many functions essential for vision in its location between the neural retina and choroid (Strauss, 2005). The RPE nourishes and supports photoreceptors by regulating transport of nutrients, ions, and water to and from the subretinal space; by maintaining the blood–retinal barrier; by re-isomerizing all-trans-retinol to 11-cis-retinal as part of the visual cycle; and by phagocytizing photoreceptor outer segment tips (Bharti et al., 2011; Saari, 2000; Strick et al., 2009). RPE dysfunction is associated with both wet and dry age-related macular degeneration (AMD), which is a leading cause of irreversible blindness in the elderly population (Zarbin, 2004).

Mouse models with altered gene expression have been critical to understanding the functions of the RPE in health and disease (Sparrow et al., 2010; Veleri et al., 2015). The Cre-loxP system is the most widely used genetic tool to generate tissue-specific gene knockouts in mice (Nagy, 2000). Driven by a tissue-selective promoter, Cre can be used to study cell-autonomous gene function. This strategy is indispensable, especially in the study of the eye due to the variety of ocular cell types (Bosenberg et al., 2006). A number of mouse lines express constitutive Cre activity in the RPE and other pigmented cells including those utilizing regulatory regions from the mouse tyrosinase-related protein 1 (*Tyrp1*), dopachrome tautomerase (*Dct*), melan-A (*Mlana*), or human bestrophin1 (*BEST1*) genes (Iacovelli et al., 2011; Mori et al., 2002; Guyonneau et al., 2002; Aydin et al., 2011). The *Tyrp1-Cre*, *Mlana-Cre* and *Dct-Cre* transgenes are useful for modulating gene expression during embryonic development, but their utility for studying postnatal processes in the context of an otherwise normal retina is limited because of the importance of the RPE to retinal development (Fuhrmann et al., 2014). While the *BEST1-Cre* mouse line exhibits postnatal expression, the pattern is mosaic, ranging from 90% to < 20% of RPE cells, and expression is often variable even among littermates (Iacovelli et al., 2011; Swarup et al., 2019).

In addition to the spatial control afforded by cell and tissue selective regulatory elements, temporal control of Cre-mediated recombination can also be useful (Nagy, 2000). Two genetic tools, tamoxifen inducible and tetracycline inducible Cre recombinase, have been most commonly used to achieve temporal regulation (Saunders, 2011; Ledbetter et al., 2014). Both systems have been applied to the RPE. In the tamoxifen system, Cre recombinase is fused to a human mutant estrogen receptor ligand-binding domain (CreERT2) and is activated by the estrogen antagonist 4-hydroxytamoxifen (4OHT) (Saunders, 2011). A line with CreERT2 driven by *Mct3* regulatory sequences exhibits limited Cre activity, detected in only about 20% of RPE cells (Longbottom et al., 2009). A line with CreERT2 driven by *Tyr* regulatory sequences has higher recombination rates in both adult (47–69%) and embryonic (~83%) RPE, but also in nearly 11% of ciliary body cells and in the inner nuclear layer with no cell type-specificity documented (Schneider et al., 2018). A *Tyrp1-CreERT2* line showed activity in 40–80% of central RPE cells and in numerous epithelial cells of the iris and ciliary body, as well as in scattered cells in the neural retina (Mori et al., 2012). Another line used a 2.9-kb fragment of the human *BEST1* promoter to drive expression of the reverse Tet-inducible transactivator protein to control a Cre open reading frame positioned downstream of a tetracycline-responsive element (Le et

al., 2008). Cre expression in this line has been reported to be leaky (i.e. independent of inducer) and present in a maximum of only 60% of RPE cells (Sundermeier et al., 2017; Fu et al., 2014). Thus, existing RPE-selective constitutive and inducible Cre driver lines suffer from various factors that limit utility. We sought to address these shortcomings and create a mouse line with robust postnatal spatial and temporal regulation of Cre recombinase activity in the RPE.

2. Materials and methods

2.1. Generation of a transgenic *Rosa26*$^{BEST1\text{-}CreERT2}$ mouse line

A *Rosa26*$^{BEST1\text{-}CreERT2}$ mouse line was generated by joining ERT2 with the open reading frame of the *BEST1*-Cre plasmid previously described (see Supplementary Document 1 for the sequence of the construct used here) (Iacovelli et al., 2011). The targeting plasmid was constructed by inserting the *BEST1*-CreERT2 construct between the two attB sites of pBT378. Pronuclei of C57BL/6J (B6) *Rosa26* $^{attPx3/attPx3}$ zygotes were injected with the *BEST1*-CreERT2 targeting plasmid and capped ϕC31 integrase mRNA (Tasic et al., 2011). Injected zygotes were then implanted into pseudopregnant CD1 females.

2.2. Animals

All experiments had ethical approval from the Stanford Institutional Animal Care and Use Committee and were in accordance with the ARVO Statement for the Use of Animals in Ophthalmic and Vision Research guidelines. Mice were housed with a 12 hour light/dark cycle. B6.Cg-Gt(*ROSA)26*$^{Sortm14(CAG\text{-}tdTomato)Hze/J}$ reporter mice (JAX stock #007914, referred to as Ai14) were crossed with *Rosa26*$^{BEST1\text{-}CreERT2}$ mice (Madisen et al., 2010). Cre-mediated recombination of the lox stop lox cassette (LSL) enabled us to visualize Cre activity in the RPE by observing red fluorescence from tdTomato.

2.3. Genotyping for *Rosa26* $^{BEST1\text{-}CreERT2}$

Mice were genotyped for the *BEST1*-CreERT2 transgene by PCR analysis of tail DNA with primers forward: 5’-ATG CCC AAG AAG AAG AGG AAG GTG TCC-3’ and reverse: 5’-GGA AAA TGC CAA TGC TCT GT-3’. PrimerSTAR GXL DNA polymerase and reagents (Takara) were used to amplify ~2-kb product (30s at 98°C for initial denaturation, 40 cycles of 30s at 98°C for denaturation, 30s at 60°C for annealing, 2 min at 68°C for extension, and finally 5 min at 68°C for final extension). The PCR product was separated on a 1.5% agarose gel.

2.4. Induction of Cre recombinase activity

To prepare injectable tamoxifen, 50 mg of 4OHT (Sigma-Aldrich) was first dissolved in 3 ml ethanol by sonication. A volume of 180 μl of the 4OHT ethanol solution was mixed well with 900 μl of filtered corn oil by vortexing, and then centrifuged at 1000 × g for 30 min under vacuum to remove the ethanol. The 4OHT stock solution and oil-dissolved 4OHT were used within 36 hours of preparation. To induce Cre recombinase activity, 4OHT was administered via four consecutive daily intraperitoneal (IP) injections of 30 mg/kg or 60 mg/kg.

2.5. Assessment of *Rosa26*$^{BEST1\text{-}CreERT2}$-mediated ablation of *Tfam*

The *Rosa26*$^{BEST1\text{-}CreERT2}$ allele was crossed into mice homozygous for a floxed allele of *Tfam* (Larsson et al., 1998). Mice injected with 4OHT were euthanized at various times post injection, and eyes were immediately enucleated. The anterior segment was removed and neural retina was peeled off. The remaining eyecup was then placed directly into ATL buffer (Qiagen, Valencia, CA) and RPE cells were collected by pipetting and centrifuging at 1000 × g. DNA was separately extracted from RPE, neural retina and choroid/sclera (QIAamp DNA Micro Kit; Qiagen, Valencia, CA) (Iacovelli et al., 2011). Primers for *Tfam* genotyping have been previously described (Larsson et al., 1998). DNA was amplified using Taq DNA polymerase (DreamTaq; Fermentas Life Sciences, Glen Burnie, MD) as recommended by the manufacturer.

2.6. Immunofluorescence

Anesthetized mice were sacrificed by cervical dislocation and their eyes were immediately removed. Eyes were marked for orientation by punching a hole in the temporal surface of the cornea. Eyeballs were first fixed in 4% paraformaldehyde for 30 minutes at 4°C. Then dissected globes were fixed for 2 hours at 4°C and rinsed 3 times with PBS. Other tissues were fixed overnight in 4% paraformaldehyde at 4°C. Dissected eyecups or other tissues were cryoprotected in 30% sucrose. After embedding in optimal cutting temperature compound (Tissue-Tek; Sakura Finetek, Torrance, CA), 12 μm-thick cryosections were taken. Immunofluorescence was performed on cryosections or retina flatmounts as previously described (Vollrath et al., 2015). Alexa Fluor™ 488 Phalloidin (1:400; Invitrogen) and primary antibodies to mouse SOX9 (1:100 dilution; AB5535; Millipore) and glutamine synthetase (1:400 dilution; AB49873; Abcam) were used. Goat anti-rabbit Alexa Fluor™ 488 (1:400; Invitrogen) was used as a secondary antibody. Fluoromount-G (SouthernBiotech) was used to mount flatmounts or cryosections on slides to examine fluorescence.

2.7. Optical coherence tomography (OCT)

A Spectralis™ HRA + OCT device (Heidelberg Engineering, Heidelberg, Germany) was used to evaluate retinal structural changes. Mice were anesthetized by IP injection of xylazine (10 mg/kg body weight), ketamine (25 mg/kg body weight) and imaged between 12 and 3 PM. After anesthetizing, eyes were dilated with 2.5% phenylephrine and 1% tropicamide (Mydriaticum Stulln; Pharma Stulln GmbH, Stulln, Germany). Hard contact lenses were applied to protect the cornea and GONAK (2.5% hypromellose ophthalmic demulcent solution, ARKON) was used as a lubricant. The optic nerve head was aligned to the center of the OCT image. Heidelberg Eye Explorer Software was used to calculate the mean retinal thickness from the eight quadrants around the optic nerve head.

2.8. Electroretinography

Electroretinography (ERG) data collection and analysis for a- and b-waves were done as previously described (Benchorin et al., 2017). The c-wave was measured with a Celeris Full-Field system (Diagnosys LLC) according to the manufacturer's instructions. For light

stimulation and calibration of light stimuli, a previously described method was used (Zhao et al., 2011).

2.9. Image analysis

Images were processed using FIJI software (https://imagej.net/Fiji/Downloads). For quantification of Cre activity using the tdTomato reporter, the area of red fluorescence divided by the total area of an RPE flatmount was calculated and converted to a percentage value.

2.10. Statistics

Student's t-test and one-way ANOVA were performed for statistical analysis using GraphPad Prism 5. $P < 0.05$ was considered statistically significant.

3. Results

3.1. Generation of *Rosa26* $^{BEST1\text{-}CreERT2}$ transgenic mice

An attractive starting point for our efforts was the widely used *BEST1-Cre* transgene, which can support robust RPE-selective expression albeit with variable mosaicism. We surmised that the mosaicism arises from epigenetic silencing of the repetitive array of five transgene copies at the integration site (Cain-Hom et al., 2017). We sought to remedy this by integrating a single copy of a construct in a defined, favorable chromosomal location through ϕC31 site-specific integrase-mediated transgenesis (Tasic et al., 2011). To achieve temporal regulation, we used the well tested CreERT2 fusion (Feil et al., 1997; Shimshek et al., 2002) (Fig. 1A), which has been employed to good effect in mouse rods (Koch et al., 2015). We targeted integration to the *Rosa26* locus because long experience has shown that it can support high levels of transgene expression in a variety of tissues across a range of ages. We also incorporated three SV40 polyadenylation signals upstream of the *BEST1* promoter fragment to mitigate interference from the endogenous *Rosa26* promoter.

We verified correct transgene integration in two founders and crossed each to B6 mice to assess germline transmission. A female founder passed the *Rosa26*$^{BEST1\text{-}CreERT2}$ allele to about 50% of her offspring, with no evidence of other sites of integration by PCR using primers located within the construct. F1 mice were crossed to Ai14 reporter mice with a Cre-conditional allele of tdTomato integrated at *Rosa26* to generate *Rosa26* $^{BEST1\text{-}CreERT2/\ LSL\text{-}tdTomato}$ mice (Madisen et al., 2010). As expected from the C57BL/6J parentage, these mice did not harbor the *rd8* allele of the *Crb1* gene (data not shown).

3.2. *Rosa26* $^{BEST1\text{-}CreERT2}$ confers robust induced RPE-selective Cre activity over a range of ages

We tested several dosing protocols to identify a suitable method for postnatal induction of Cre recombinase activity. We chose to use 4OHT and bypass the requirement for hepatic metabolism of tamoxifen. We qualitatively assessed the extent of tdTomato fluorescence in male *Rosa26* $^{BEST1\text{-}CreERT2/\ LSL\text{-}tdTomato}$ mice injected IP with two to five consecutive daily doses (30 mg per kg) beginning at P14. Fundus imaging four weeks post injection revealed increasing fluorescence with additional daily doses (Fig. S1A). Four doses resulted in

tdTomato fluorescence in a large majority of the visible retina. Five doses showed a similar high level of fluorescence in the RPE, but with increased neural retinal fluorescence (Fig. S1B). We also delivered 4OHT as eye drops in corn oil (0.05 mg in 10 ul) and assessed the qualitative effects by fundus imaging (two consecutive daily doses beginning at 7 weeks) or by fluorescence imaging of an RPE/choroid sclera wholemount (five consecutive daily doses beginning at P14). Both protocols resulted in obvious but low level activation of Cre recombination (data not shown). We did not test intravitreal injection of 4OHT because of concerns that a single dose would not be sufficient and that repeated daily injections could damage the eye.

In light of our qualitative findings, we selected a protocol of four consecutive daily IP injections. We quantified the percentage of the area of RPE/choroid/sclera flatmounts exhibiting tdTomato fluorescence from *Rosa26* $^{BEST1\text{-}CreERT2}$/ $^{LSL\text{-}tdTomato}$ mice injected beginning at P14. Induction of recombination was highly efficient; males exhibited fluorescence across 90.7±4.5% (mean±S.E.) of the flatmount and females across 84.7±3.2% (Fig. 1B and C). Robust induction was also achieved in mice as old as 7 weeks (males 84.3±7.0%, females 82±3.6%) at twice the daily dose used at P14 (Fig. 1B and C).

To assess the cell-type specificity of Cre activity, we examined a continuous series of retinal sagittal sections from a male induced beginning at P14. tdTomato fluorescence is evident throughout the RPE, from the center to periphery and across the full width of the eyeball (Fig. 2A and S2). No fluorescence was seen in the choroid or sclera (Fig. 1D), confirming the RPE origin of the flatmount fluorescence. We saw no fluorescence above background in the anterior segment of the eye (data not shown) or in the brain, heart, kidney, muscle, liver, lung and spleen. However, we did observe a low level of Cre-mediated recombination in the testis (Fig. 2A). Together, these data indicate that the *Rosa26* $^{BEST1\text{-}CreERT2}$ transgene confers robust and selective induction of Cre activity throughout the RPE across a range of postnatal ages.

3.3. *Rosa26* $^{BEST1\text{-}CreERT2}$ expresses inducible Cre activity in a small fraction of Muller glia

Examination of retinal sections from induced mice revealed sparse tdTomato signals within the neural retina (Fig. 1D and 2B). The nature of the signals, present in multiple retinal layers with occasional streaks oriented perpendicular to the laminae (Fig. 1D), suggested that they may derive from Muller glia. Indeed, these sparse tdTomato signals co-localized in frozen sections with the Muller cell marker glutamine synthetase (Fig. 3A). The Muller glial origin of the signals was confirmed by co-localization in neural retinal flatmounts with a second marker, SOX9 (Fig. 3B). We quantified the percentage of SOX9 positive Muller glia with co-localized tdTomato signals across eight regions of neural retinal flatmounts demarcated by central to peripheral, superior to inferior, and nasal to temporal axes. A small fraction of Muller glia exhibited 4OHT dependent tdTomato expression in males and females injected beginning at P14 (<0.3%) and 7 weeks (<0.6%) (Fig. 3C). No bias in expression to a particular retinal region was apparent. The slightly higher Muller glial induction at 7 weeks is consistent with the higher daily dose of 4OHT (60 mg/kg). Males

injected daily at 7 weeks with 30 mg/kg 4OHT had <0.3% tdTomato positive Muller glia, similar to the same dose at P14 (data not shown).

3.4. No evidence of retinal toxicity in *Rosa26* $^{BEST1\text{-}CreERT2}$ homozygotes

To assess possible retinal toxicity associated with *Rosa26* $^{BEST1\text{-}CreERT2}$, age matched male *Rosa26* $^{BEST1\text{-}CreER2T/BEST1\text{-}CreERT2}$ and B6 mice were treated with 4OHT or vehicle at P14. Mean retinal thickness was similar between *Rosa26* $^{BEST1\text{-}CreER2T/BEST1\text{-}CreERT2}$ and controls at 7 months of age as measured by OCT (Fig. 4A and B). There was no apparent difference in RPE morphology or cell size (Fig. 4C and D). Scotopic a-, b- and c-wave amplitudes also were not statistically distinguishable 10 months after induction (Fig. 4E to I). Thus, the *Rosa26* $^{BEST1\text{-}CreERT2}$ transgene is associated with no obvious retinal toxicity, even in the homozygous state.

3.5. *Rosa26* $^{BEST1\text{-}CreERT2}$ -mediated ablation of *Tfam* degrades retinal structure and function

To demonstrate the utility of *Rosa26* $^{BEST1\text{-}CreERT2}$ to modulate gene function in the postnatal RPE, we generated mice heterozygous for the transgene and homozygous for a Cre-conditional (floxed) allele of *Tfam*, which encodes a protein necessary for the transcription and replication of the mitochondrial genome (Larsson et al., 1998). Male mice induced beginning at P14 displayed efficient and RPE-selective ablation of *Tfam* (Fig. 5A). Mean retinal thickness was significantly reduced in induced 8-month-old *Rosa26* $^{BEST1\text{-}CreERT2}$; Tfam fl/fl animals compared to 4OHT injected littermates lacking the transgene (Fig. 5B and C). Scotopic a- and b-wave amplitudes were also significantly reduced in the same induced transgenic animals at 12 months of age across a range of stimulus luminances (Fig. 5D to F). These findings are consistent with the reduced outer nuclear layer thickness and diminished scotopic a- and b-wave amplitudes documented in 9-month-old RPEΔ*Tfam* mice generated with the constitutive *BEST1-Cre* transgene (Zhao et al., 2011).

4. Discussion

Motivated by an interest in modeling human age-related photoreceptor degeneration in mice, we achieved our goal of creating a Cre driver line suitable for modulating RPE gene expression postnatally. The *Rosa26* $^{BEST1\text{-}CreERT2}$ allele allowed consistent induction of Cre activity in a large proportion of RPE cells, removing the requirement to use one eye of each animal to assess the level of Cre expression, as we routinely do for *BEST1-Cre* transgenics. Moreover, as with other Cre driver lines, the *BEST1-Cre* transgene can cause germline recombination of Cre-conditional alleles, producing offspring in which Cre-mediated recombination has occurred throughout the animal (Iacovelli et al., 2011; Song, 2018). Breeding uninduced *Rosa26* $^{BEST1\text{-}CreERT2}$ mice largely avoids this problem, although we did observe germline recombination of a Cre-conditional *Tfam* allele at a frequency of ~1% in the offspring of an uninjected transgene positive male. Combined, these factors substantially increase the quality and quantity of mice in each litter available for experiments.

We observed robust induction of Cre activity in animals as old as 7 weeks. Germline or early postnatal knockouts have been used to probe the necessity of genes related to dynamic RPE processes such as phagocytosis of photoreceptor outer segments, the visual cycle, and transport of ions and metabolites. Our results open the way for timed modulation of such functions in older animals, expanding the range of hypotheses that can be tested and perhaps leading to revised genotype/phenotype correlations. For example, genetic compensation occurring during the embryonic to early postnatal period can confound assessment of loss of function phenotypes, but is not prevalent in knockouts initiated at later ages (El-Brolosy et al., 2017).

Abnormalities in RPE monolayer morphology have been reported for 8-month-old mice homozygous for the *BEST1-Cre* transgene, but no abnormalities were detected in heterozygous animals at two years of age (Iacovelli et al., 2011; He et al., 2014). We found no evidence of RPE or rod toxicity in 7 to 10-month-old mice homozygous for the *Rosa26* $^{BEST1\text{-}CreERT2}$ transgene. Given the robust Cre activity achievable with a single *Rosa26* $^{BEST1\text{-}CreERT2}$ allele, homozygous animals should not be needed. Except for the rare germline recombinant previously noted, we did not detect tamoxifen independent induction of Cre activity like that reported for some non-ocular CreERT2 lines, nor did we see evidence of tamoxifen induced retinal toxicity (Álvarez-Aznar et al., 2020, Lindhorst et al., 2020). In fact, tamoxifen has been reported to be non-toxic to the murine retina and may even be beneficial (Boneva et al., 2016; Wang, X et al., 2017). We did note a trend toward lower induction of Cre activity in the RPE of females compared to males at both ages, consistent with the lower induction in females reported for a *Tyr-CreERT2* line (Schneider et al., 2018). The sex-based differences in induction we saw were relatively small and could be overcome at seven weeks by doubling the dose of tamoxifen.

Our observation of Cre activity in a small fraction of Muller glia is not surprising. A larger *BEST1* promoter fragment than the one we used is capable of driving expression exclusively in Muller glia (Ueki et al., 2009). Moreover, SOX9 activates the *BEST1* promoter in the RPE and is also abundantly expressed in Muller glia (Masuda et al., 2010; Wang, J et al., 2017). The combination of robust Cre activity in the RPE and trace expression in Muller glia suggests that retinal phenotypes observed in conjunction with the *Rosa26* $^{BEST1\text{-}CreERT2}$ transgene can be ascribed to modulation of gene function in the RPE. This assertion is supported by the similarities in the retinal phenotypes of mice with RPE-selective knockout of *Tfam* generated with the *Rosa26* $^{BEST1\text{-}CreERT2}$ allele and those generated with the original *BEST1-Cre* transgene (Zhao et al., 2011). Overall, we expect the *Rosa26* $^{BEST1\text{-}CreERT2}$ line and the induction protocol we describe to speed efforts to create and study mice with postnatal RPE-selective loss and gain of gene function.

Supplementary Material

Refer to Web version on PubMed Central for supplementary material.

Acknowledgments

We thank Dr. Monte Winslow for providing mice with the tdTomato reporter allele, the animal care personnel at Stanford for their unwavering commitment, and the expert reviewers for critiques that improved our manuscript.

Funding: This work was supported by the National Institutes of Health [R01EY025790, P30EY026877]

Abbreviations:

LSL	lox stop lox
4OHT	4-hydroxytamoxifen

References:

Álvarez-Aznar A, Martínez-Corral I, Daubel N, Betsholtz C, Mäkinen T and Gaengel K, 2020 Tamoxifen-independent recombination of reporter genes limits lineage tracing and mosaic analysis using CreER(T2) lines. Transgenic Res. 29, 53–68. [PubMed: 31641921]

Aydin IT, Beermann F, 2011 A mart-1::Cre transgenic line induces recombination in melanocytes and retinal pigment epithelium. Genesis 49, 403–409. [PubMed: 21309074]

Benchorin G, Calton MA, Beaulieu MO, Vollrath D, 2017 Assessment of Murine Retinal Function by Electroretinography. Bio Protoc.. 7.

Bharti K, Miller SS, Arnheiter H, 2011 The new paradigm: retinal pigment epithelium cells generated from embryonic or induced pluripotent stem cells. Pigment Cell Melanoma Res. 24, 21–34. [PubMed: 20846177]

Boneva SK, Groß TR, Schlecht A, Schmitt SI, Sippl C, Jägle H, Volz C, Neueder A, Tamm ER, Braunger BM, 2016 Cre recombinase expression or topical tamoxifen treatment do not affect retinal structure and function, neuronal vulnerability or glial reactivity in the mouse eye. Neuroscience 325, 188–201. [PubMed: 27026593]

Bosenberg M, Muthusamy V, Curley DP, Wang Z, Hobbs C, Nelson B, Nogueira C, Horner JW 2nd, Depinho R, Chin L, 2006 Characterization of melanocyte-specific inducible Cre recombinase transgenic mice. Genesis 44, 262–267. [PubMed: 16676322]

Cain-Hom C, Splinter E, van Min M, Simonis M, van de Heijning M, Martinez M, Asghari V, Cox JC, Warming S, 2017 Efficient mapping of transgene integration sites and local structural changes in Cre transgenic mice using targeted locus amplification. Nucleic Acids Res. 45, e62. [PubMed: 28053125]

El-Brolosy MA, Stainier DYR, 2017 Genetic compensation: A phenomenon in search of mechanisms. PLoS Genet. 13, e1006780. [PubMed: 28704371]

Feil R, Wagner J, Metzger D, Chambon P, 1997 Regulation of Cre recombinase activity by mutated estrogen receptor ligand-binding domains. Biochem. Biophys. Res. Commun 237, 752–757. [PubMed: 9299439]

Fu S, Zhu M, Wang C, Le YZ, 2014 Efficient induction of productive Cre-mediated recombination in retinal pigment epithelium. Mol. Vis 20, 480–487. [PubMed: 24744608]

Fuhrmann S, Zou C, Levine EM, 2014 Retinal pigment epithelium development, plasticity, and tissue homeostasis. Exp. Eye. Res 123: 141–150. [PubMed: 24060344]

Guyonneau L, Rossier A, Richard C, Hummler E, Beermann F, 2002 Expression of Cre recombinase in pigment cells. Pigment Cell Res. 15, 305–309. [PubMed: 12100497]

He L, Marioutina M, Dunaief JL, Marneros AG, 2014 Age- and gene-dosage-dependent cre-induced abnormalities in the retinal pigment epithelium. Am. J. Pathol 184, 1660–1667. [PubMed: 24854863]

Iacovelli J, Zhao C, Wolkow N, Veldman P, Gollomp K, Ojha P, Lukinova N, King A, Feiner L, Esumi N, Zack DJ, Pierce EA, Vollrath D, Dunaief JL, 2011 Generation of Cre transgenic mice with postnatal RPE-specific ocular expression. Invest. Ophthalmol. Vis. Sci 52, 1378–1383. [PubMed: 21212186]

Koch SF, Tsai YT, Duong JK, Wu WH, Hsu CW, Wu WP, Bonet-Ponce L, Lin CS, Tsang SH, 2015 Halting progressive neurodegeneration in advanced retinitis pigmentosa. J. Clin. Invest 125, 3704–3713. [PubMed: 26301813]

Larsson NG, Wang J, Wilhelmsson H, Oldfors A, Rustin P, Lewandoski M, Barsh GS, Clayton DA, 1998 Mitochondrial transcription factor A is necessary for mtDNA maintenance and embryogenesis in mice. Nat. Genet 18, 231–236. [PubMed: 9500544]

Le YZ, Zheng W, Rao PC, Zheng L, Anderson RE, Esumi N, Zack DJ, Zhu M, 2008 Inducible expression of cre recombinase in the retinal pigmented epithelium. Invest. Ophthalmol. Vis. Sci 49, 1248–1253. [PubMed: 18326755]

Ledbetter DJ, Thomson JG, Piedrahita JA, Rucker EB, 2014 5 - Gene Targeting in Embryonic Stem Cells, II: Conditional Technologies Transgenic Animal Technology (Third Edition). Pinkert CA. London, Elsevier, 141–165.

Lindhorst A, Bechmann I, Gericke M, 2020 Unspecific DNA recombination in AdipoqCre-ER(T2) - mediated knockout approaches in transgenic mice is sex-, age- and genotype-dependent. Adipocyte 9, 1–6. [PubMed: 31842670]

Longbottom R, Fruttiger, Fruttiger M, Douglas RH, Martinez-Barbera JP, Greenwood J, Moss SE, 2009 Genetic ablation of retinal pigment epithelial cells reveals the adaptive response of the epithelium and impact on photoreceptors. Proc. Natl. Acad. Sci. U. S. A106, 18728–18733. [PubMed: 19850870]

Madisen L, Zwingman TA, Sunkin SM, Oh SW, Zariwala HA, Gu H, Ng LL, Palmiter RD, Hawrylyc z M.J., Jones AR, Lein ES, Zeng H, 2010 A robust and high-throughput Cre reporting and characterization system for the whole mouse brain. Nat. Neurosci 13, 133–140. [PubMed: 20023653]

Masuda T, Esumi N, 2010 SOX9, through interaction with microphthalmia-associated transcription factor (MITF) and OTX2, regulates BEST1 expression in the retinal pigment epithelium. J. Biol. Chem 285, 26933–26944. [PubMed: 20530484]

Mori M, Gargowitsch L, Bornert JM, Garnier JM, Mark M, Chambon P, Metzger D, 2012 Temporally controlled targeted somatic mutagenesis in mouse eye pigment epithelium. Genesis 50, 828–832. [PubMed: 22730183]

Mori M, Metzger D, Garnier JM, Chambon P, Mark M, 2002 Site-specific somatic mutagenesis in the retinal pigment epithelium. Invest. Ophthalmol. Vis. Sci 43, 1384–1388. [PubMed: 11980850]

Nagy A, 2000 Cre recombinase: the universal reagent for genome tailoring. Genesis 26, 99–109. [PubMed: 10686599]

Saari JC, 2000 Biochemistry of visual pigment regeneration: the Friedenwald lecture. Invest. Ophthalmol. Vis. Sci 41, 337–348. [PubMed: 10670460]

Saunders TL, 2011 Inducible transgenic mouse models. Methods Mol. Biol 693, 103–115. [PubMed: 21080277]

Schneider S, Hotaling N, Campos M, Patnaik SR, Bharti K, May-Simera HL, 2018 Generation of an inducible RPE-specific Cre transgenic-mouse line. PLoS One 13, e0207222. [PubMed: 30440011]

Shimshek DR, Kim J, Hübner MR, Spergel DJ, Buchholz F, Casanova E, Stewart AF, Seeburg PH, Sprengel R, 2002 Codon-improved Cre recombinase (iCre) expression in the mouse. Genesis 32, 19–26. [PubMed: 11835670]

Song AJ, Palmiter RD, 2018 Detecting and Avoiding Problems When Using the Cre-lox System. Trends Genet. 34, 333–340. [PubMed: 29336844]

Sparrow JR, Hicks D, Hamel CP, 2010 The retinal pigment epithelium in health and disease. Curr. Mol. Med 10, 802–823. [PubMed: 21091424]

Strauss O, 2005 The retinal pigment epithelium in visual function. Physiol. Rev 85, 845–881. [PubMed: 15987797]

Strick DJ, Feng W and Vollrath D, 2009 Mertk drives myosin II redistribution during retinal pigment epithelial phagocytosis. Invest. Ophthalmol. Vis. Sci 50, 2427–2435. [PubMed: 19117932]

Sundermeier TR, Sakami S, Sahu B, Howell SJ, Gao S, Dong Z, Golczak M, Maeda A, Palczewski K, 2017 MicroRNA-processing Enzymes Are Essential for Survival and Function of Mature Retinal Pigmented Epithelial Cells in Mice. J. Biol. Chem 292, 3366–3378. [PubMed: 28104803]

Swarup A, Samuels IS, Bell BA, Han JYS, Du J, Massenzio E, Abel ED, Boesze-Battaglia K, Peachey NS, Philp NJ, 2019 Modulating GLUT1 expression in retinal pigment epithelium decreases glucose levels in the retina: impact on photoreceptors and Müller glial cells. Am. J. Physiol. Cell Physiol 316, C121–c133. [PubMed: 30462537]

Tasic B, Hippenmeyer S, Wang C, Gamboa M, Zong H, Chen-Tsai Y, Luo L, 2011 Site-specific integrase-mediated transgenesis in mice via pronuclear injection. Proc. Natl. Acad. Sci. U. S. A 108, 7902–7907. [PubMed: 21464299]

Ueki Y, Ash JD, Zhu M, Zheng L, Le YZ, 2009 Expression of Cre recombinase in retinal Müller cells. Vision Res. 49, 615–621. [PubMed: 19948109]

Veleri S, Lazar CH, Chang B, Sieving PA, Banin E, Swaroop A, 2015 Biology and therapy of inherited retinal degenerative disease: insights from mouse models. Dis. Model Mech 8, 109–129. [PubMed: 25650393]

Vollrath D, Yasumura D, Benchorin G, Matthes MT, Feng W, Nguyen NM, Sedano CD, Calton MA, LaVail MM, 2015 Tyro3 Modulates Mertk-Associated Retinal Degeneration. PLoS Genet. 11, e1005723. [PubMed: 26656104]

Wang J, O'Sullivan ML, Mukherjee D, Puñal VM, Farsiu S, Kay JN, 2017 Anatomy and spatial organization of Müller glia in mouse retina. J. Comp. Neurol 525, 1759–1777. [PubMed: 27997986]

Wang X, Zhao L, Zhang Y, Ma W, Gonzalez SR, Fan J, Kretschmer F, Badea TC, Qian HH, Wong WT, 2017 Tamoxifen Provides Structural and Functional Rescue in Murine Models of Photoreceptor Degeneration. J Neurosci. 37, 3294–3310. [PubMed: 28235894]

Zarbin MA, 2004 Current concepts in the pathogenesis of age-related macular degeneration. Arch. Ophthalmol 122, 598–614. [PubMed: 15078679]

Zhao C, Yasumura D, Li X, Matthes M, Lloyd M, Nielsen G, Ahern K, Snyder M, Bok D, Dunaief JL, LaVail MM, Vollrath D, 2011 mTOR-mediated dedifferentiation of the retinal pigment epithelium initiates photoreceptor degeneration in mice. J. Clin. Invest 121, 369–383. [PubMed: 21135502]

- Consistent and robust induction of Cre activity throughout the RPE
- RPE-selective inducible Cre activity across a range of postnatal ages
- No evidence of retinal toxicity in 7-month-old transgenic homozygotes

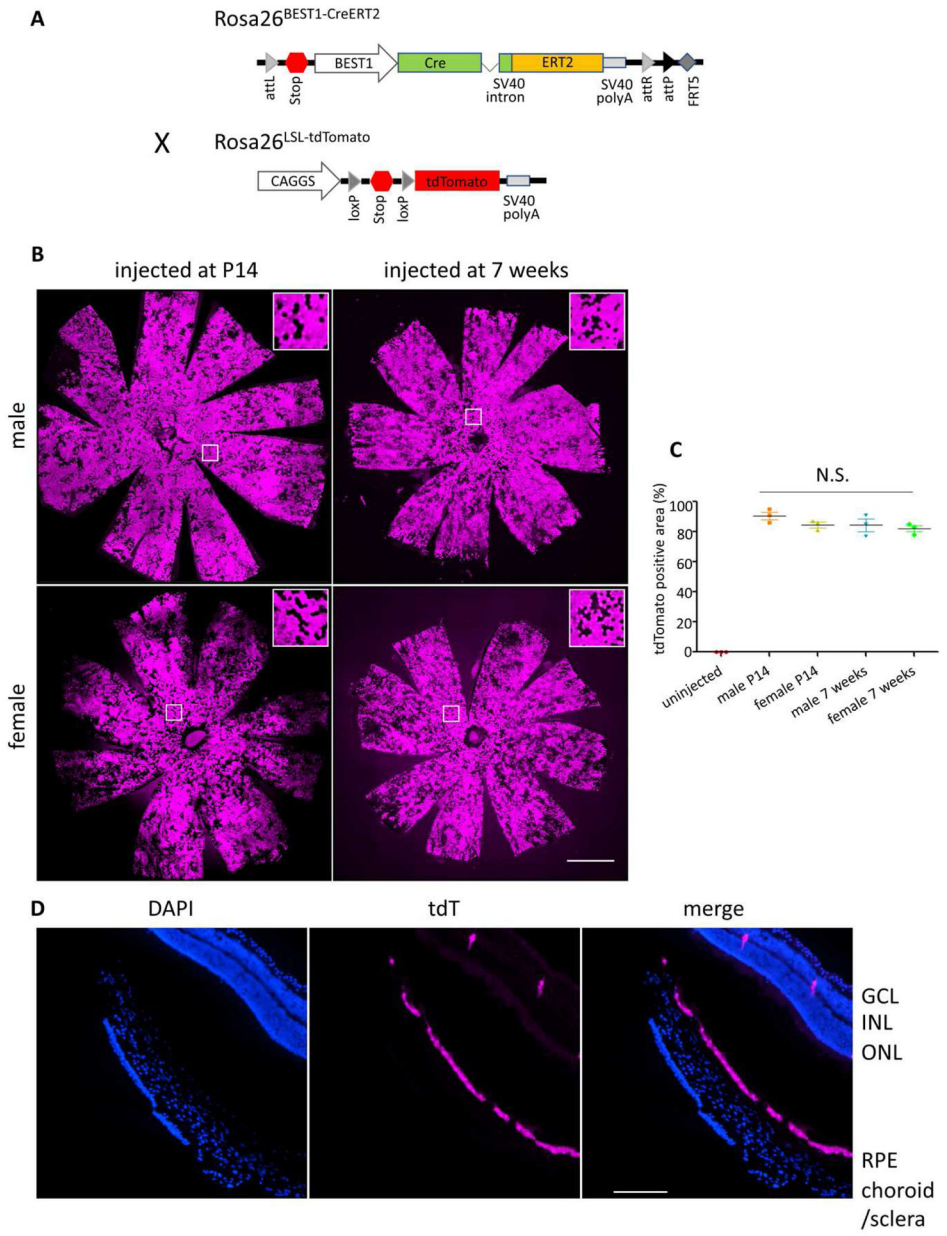

Fig. 1. Efficient induction of Cre activity in the RPE of both sexes over a range of ages

(**A**) Schematic of the DNA construct used to generate the *Rosa26*$^{BEST1\text{-}CreERT2}$ allele by ϕ C31-mediated integration. *Rosa26*$^{BEST1\text{-}CreERT2}$ mice were subsequently crossed to Ai14 mice with a Cre-conditional tdTomato reporter cassette at *Rosa26* to generate *Rosa26* $^{BEST1\text{-}CreERT2/\ LSL\text{-}tdTomato}$ mice. Cre-mediated recombination excises the stop region, enabling tdTomato expression. (**B**) tdTomato fluorescence of RPE/choroid/sclera flatmounts from *Rosa26* $^{BEST1\text{-}CreERT2/\ LSL\text{-}tdTomato}$ mice of each sex injected with 4OHT for four consecutive days beginning at P14 (30 mg/kg) or at 7 weeks of age (60 mg/kg). White boxes indicate areas of higher magnification shown in the insets. (**C**) The efficiency of induced Cre-mediated recombination was quantified as the mean ± S.E. percentage of the total RPE flatmount area that was tdTomato positive. n = 3 eyes from different animals for each

category. The efficiency was not statistically different by one-way ANOVA. (**D**) Retinal cryosection from a 4OHT treated (four 30 mg/kg injections beginning at P14) male *Rosa26*$^{BEST1\text{-}CreERT2/\ LSL\text{-}tdTomato}$ mouse. Scale bars: (B) 1000 μm, (C) 170 μm

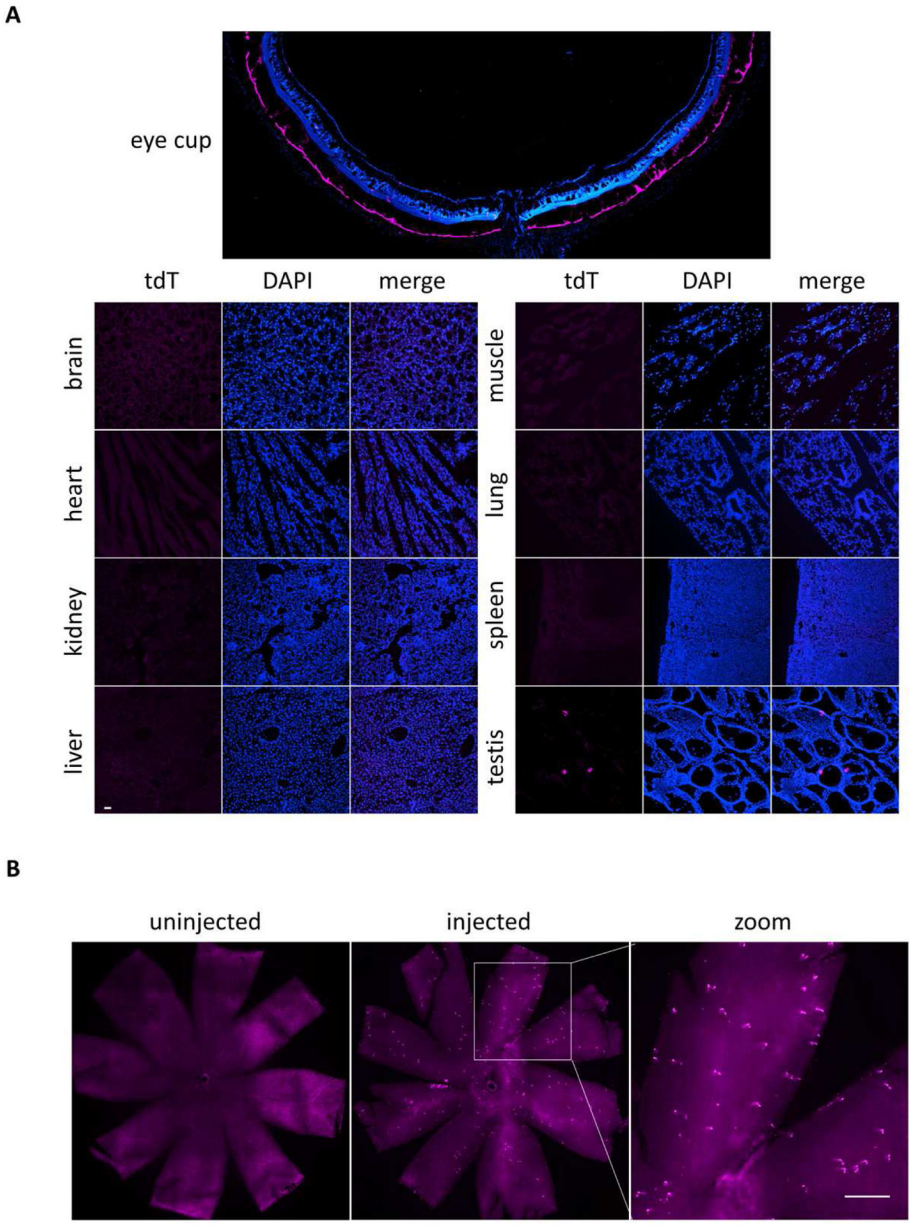

Fig. 2. Retina-selective induction of Cre activity in *Rosa26* $^{BEST1\text{-}CreERT2/\ LSL\text{-}tdTomato}$ mice

(**A**) Sagittal eyecup cryosection through the optic nerve head from a male *Rosa26* $^{BEST1\text{-}CreERT2/\ LSL\text{-}tdTomato}$ mouse injected beginning at P14 as done for Fig. 1B shows RPE-selective tdTomato fluorescence indicative of efficient Cre activity. No tdTomato fluorescence was detected in multiple tissues including brain, heart, kidney, muscle, liver, lung and spleen, with the exception of infrequent foci in the testis. (**B**) Neural retinal flatmount from a male *Rosa26* $^{BEST1\text{-}CreERT2/\ LSL\text{-}tdTomato}$ mouse treated as in (A) shows sparse foci of tdTomato expression not present in an uninjected control of the same sex and genotype. Scale bars: (A) 40 μm, (B) 300 μm.

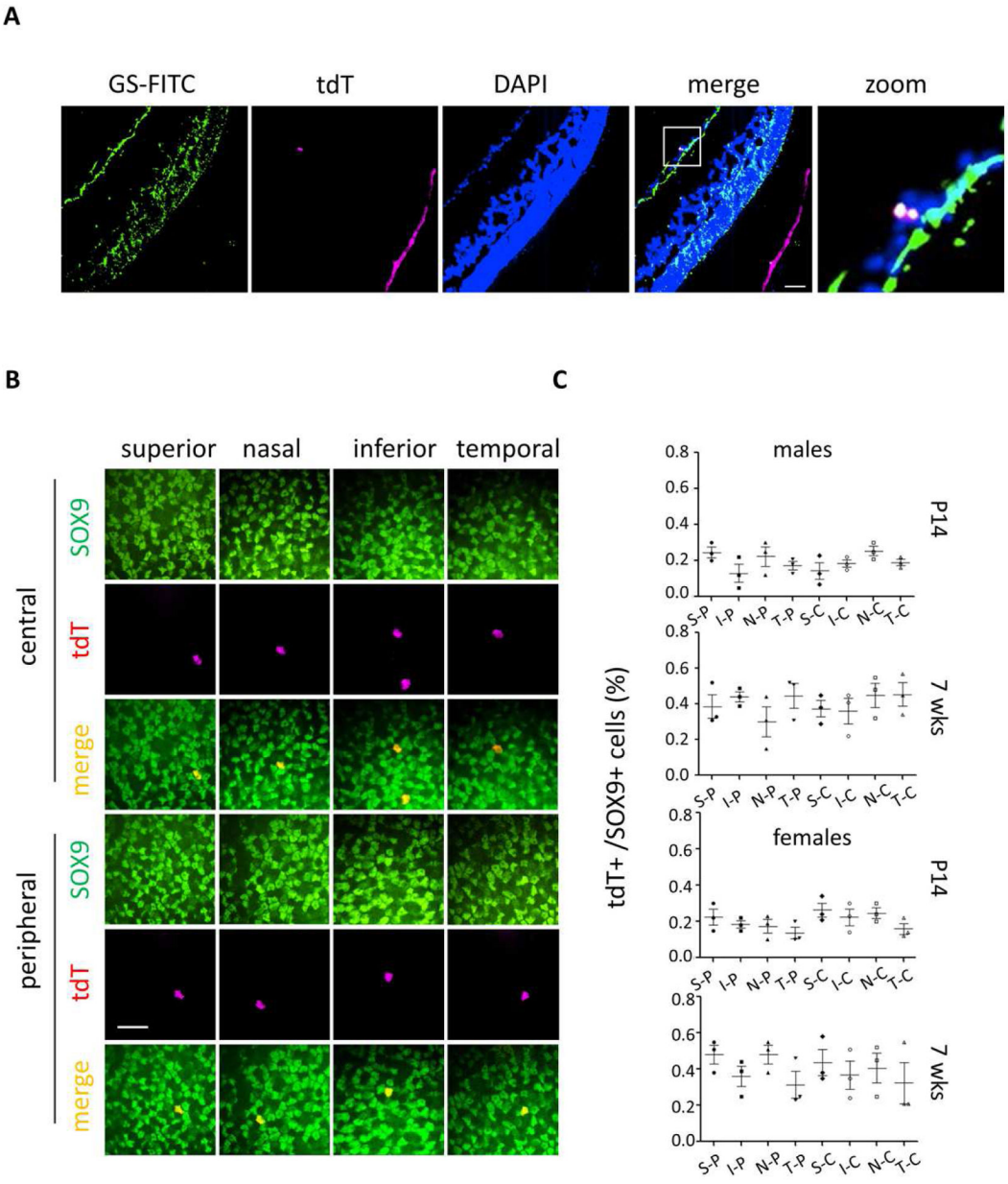

Fig. 3. Induced Cre-mediated recombination in a small fraction of Muller glia

(**A**) Glutamine synthetase (GS) immunofluorescence staining of an eyecup cryosection from a male *Rosa26* $^{BEST1\text{-}CreERT2/\ LSL\text{-}tdTomato}$ mouse treated as for Fig. 2A. (**B**) SOX9 staining of a neural retinal flatmount from a male mouse treated as for Fig. 2A. (**C**) Quantification of the mean ± S.E. percentage of SOX9 and tdTomato double positive cells in eight areas including central (C) and peripheral (P) on superior (S)/inferior (I) and nasal (N)/temporal (T) axes with treatments as described for Fig. 1B. More than 100 SOX9 positive nuclei were assessed for each of the eight areas. n = 3 independent eyes for each sex at each age. Scale bars: (A) 20 μm, (B) 10 μm.

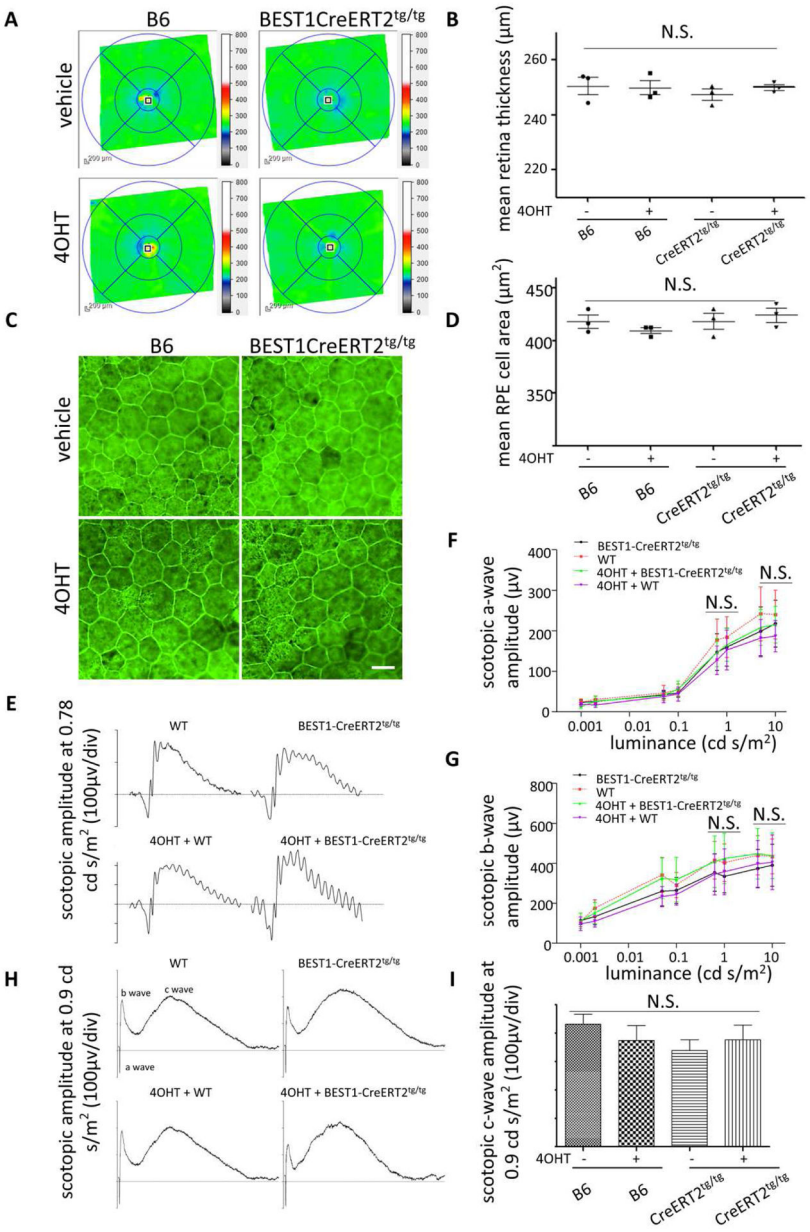

Fig. 4. Assessment of retinal toxicity in *Rosa26* $^{BEST1\text{-}CreERT2}$ homozygotes

(**A** and **B**) OCT B-scans of the retinas of 7-month-old homozygous *Rosa26*$^{BEST1\text{-}CreERT2}$ and B6 control male mice injected with 4OHT or vehicle beginning at P14 as described for Fig. 1B. No difference was observed by one-way ANOVA. (**C**) Retinal flatmounts stained with phalloidin show normal RPE morphology between *Rosa26* $^{BEST1\text{-}CreERT2}$ homozygotes and B6 mice treated as for Fig. 4A. (**D**) Mean RPE cell area calculated from images of the type shown in Fig. 4C. No difference was observed between *Rosa26* $^{BEST1\text{-}CreERT2}$ homozygotes and B6 mice with or without 4OHT treatment by one-way ANOVA. (**E to I**) Scotopic a-wave, b-wave (E, F and G) and c-wave (H and I) responses were not different among groups of 10-month-old mice by one-way ANOVA. For (B) and (D, F, G and I), n = 3 independent samples for each group. Scale bar: (B) 20 μm.

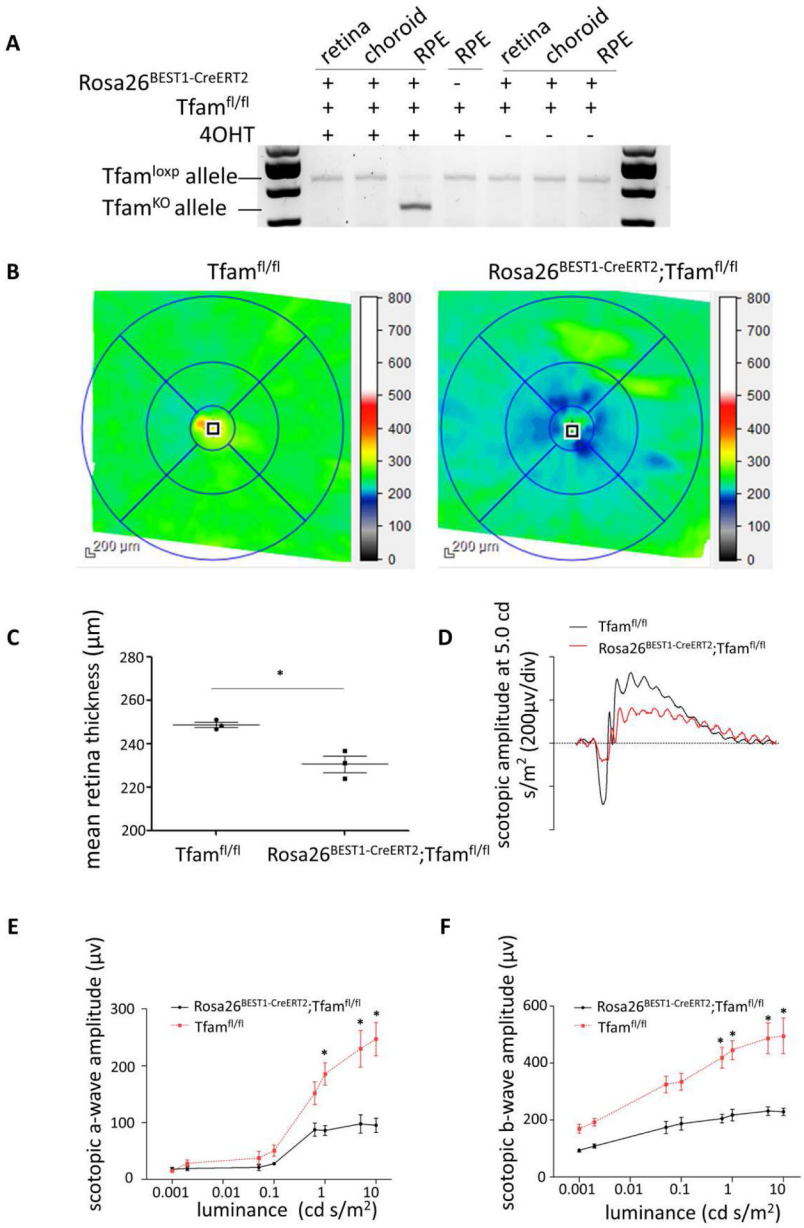

Fig. 5. Induction of retinal dysfunction in *Rosa26* $^{BEST1\text{-}CreERT2/+}$;*Tfam* $^{fl/fl}$ mice

(A) PCR genotyping of tissues from male *Rosa26* $^{BEST1\text{-}CreERT2/+}$; *Tfam* $^{fl/lfl}$ and *Tfam* $^{fl/lfl}$ mice injected with 4OHT beginning at P14 as described for Fig. 1B demonstrates efficient, RPE-selective knockout (KO) of *Tfam* for the induced transgenic animal. (**B**) OCT B-scans of the retinas of 8-month-old male *Rosa26*$^{BEST1\text{-}CreERT2/+}$; *Tfam* $^{fl/lfl}$ and *Tfam* $^{fl/lfl}$ mice treated as in Fig. 5A. (**C**) Analysis of OCT data from (B) demonstrates reduced mean retinal thickness in *Rosa26*$^{BEST1\text{-}CreERT2/+}$; *Tfam* $^{fl/lfl}$ mice (n = 3, $P = 0.02$, Students *t*-test, single tail). (**D**, **E and F**) Electroretinography demonstrates significantly reduced scotopic a-wave and b-wave responses in 12-month-old *Rosa26*$^{BEST1\text{-}CreERT2/+}$; *Tfam* $^{fl/lfl}$ mice compared to *Tfam* $^{fl/lfl}$ controls (n = 3 for each). Data are from the same animals used for (A-C). For the

scotopic a-wave, P = 0.0283; 0.0480; 0.0456 (right to left) (Students *t*-test, double tail). For the scotopic b-wave, P = 0.0493; 0.0374; 0.0129; 0.0220 (right to left).